Time-Resolved Infrared Spectroscopy of Electron Transfer in Bacterial Photosynthetic Reaction Centers: Dynamics of Binding and Interaction upon Q_A and Q_B Reduction†

R. Hienerwadel,‡ D. Thibodeau,§,‖ F. Lenz,‡ E. Nabedryk,§ J. Breton,§ W. Kreutz,‡ and W. Mäntele*,‡

Institut für Biophysik und Strahlenbiologie der Universität Freiburg, Albertstrasse 23, D-7800 Freiburg, FRG, and Section de Bioénergétique, Département de Biologie Cellulaire et Moléculaire, CEN Saclay, F-91191 Gif-sur-Yvette Cedex, France

Received January 2, 1992; Revised Manuscript Received April 1, 1992

ABSTRACT: Light-induced forward electron transfer in the bacterial photosynthetic reaction center from *Rhodobacter sphaeroides* was investigated by time-resolved infrared spectroscopy. Using a highly sensitive kinetic photometer based on a tunable IR diode laser source [Mäntele, W., Hienerwadel, R., Lenz, F., Riedel, W. J., Grisar, R., & Tacke, M. (1990a) *Spectrosc. Int. 2*, 29–35], molecular processes concomitant with electron-transfer reactions were studied in the microsecond-to-second time scale. Infrared (IR) signals in the 1780–1430-cm^{-1} spectral region, appearing within the instrument time resolution of about 0.5 μs, could be assigned to molecular changes of the primary electron donor upon formation of a radical cation and to modes of the primary quinone electron acceptor Q_A and its environment upon formation of Q_A^-. These IR signals are consistent with steady-state FTIR difference spectra of the P^+Q^- formation [Mäntele, W., Nabedryk, E., Tavitian, B. A., Kreutz, W., & Breton, J. (1985) *FEBS Lett. 187*, 227–232; Mäntele, W., Wollenweber, A., Nabedryk, E., & Breton, J. (1988) *Proc. Natl. Acad. Sci. U.S.A. 85*, 8468–8472; Nabedryk, E., Bagley, K. A., Thibodeau, D. L., Bauscher, M., Mäntele, W., & Breton, J. (1990) *FEBS Lett. 266*, 59–62] and with time-resolved FTIR studies [Thibodeau, D. L., Nabedryk, E., Hienerwadel, R., Lenz, F., Mäntele, W., & Breton, J. (1990) *Biochim. Biophys. Acta 1020*, 253–259]. At given wavenumbers, kinetic components with a half-time of approximately 120 μs were observed and attributed to $Q_A \rightarrow Q_B$ electron transfer. The time-resolved IR signals, in contrast to steady-state experiments where full protein relaxation after electron transfer can occur, allow us to follow directly the modes of Q_A and Q_B and their protein environment under conditions of forward electron transfer. Apart from signals attributed to the primary electron donor, signals are proposed to arise not only from the C=O and C=C vibrational modes of the neutral quinones and from the C—O and C—C vibrations of their semiquinone anion form but also from amino acid groups forming their binding sites. Some of the signals appearing with the instrument rise time as well as the transient 120-μs signals are interpreted in terms of binding and interaction of the primary and secondary quinone electron acceptor in the *Rb. sphaeroides* reaction center and of the conformational changes in their binding site. Since these conformational changes display kinetic parameters identical to those of the quinone modes, it appears that most of the protein relaxation processes closely follow the quinone reduction. A signal of 1617 cm^{-1}, however, manifests itself with an additional absorbance decrease component exhibiting a half-time of slightly above 1 ms. This component, which is also present with a less pronounced contribution at other frequencies, is tentatively assigned to the antisymmetric C—O vibration of a carboxylate group disappearing upon formation of the carboxylic group, presumably that of Asp L213, and attributed to a (partial) protonation upon a pK shift following a single electron reduction of Q_B.

The understanding of the sequence of events, the mechanisms of reactions, and the identity of reaction partners in the primary electron transfer of photosynthesis mainly arises from time-resolved techniques in the UV, visible, and near-IR[1] spectroscopic region [for a review, see Parson and Ke (1982)]. These primary steps of energy conversion take place in reaction centers (RC) which contain well-organized pigments and redox components. In the case of the purple photosynthetic bacterium *Rhodobacter* (*Rb.*) *sphaeroides*, these are four bacteriochlorophylls (BChl), two bacteriopheophytins (BPhe), and two acceptor quinones (Q). According to pico- and femtosecond time-resolved studies, electron transport upon photoexcitation is thought to proceed within 2–3 ps from the primary electron donor "P", a BChl *a* dimer, directly (Breton et al., 1988) or via a monomeric BChl "B" (Holzapfel et al., 1989) to the monomeric BPhe "H" and from H to the primary acceptor quinone Q_A within approximately 200 ps. In the presence of a secondary quinone, Q_B, electron transfer from Q_A to Q_B proceeds within approximately 120-μs (Wraight, 1979). If the redox energy stored in the $P^+Q_B^-$ state is not used by further electron-transfer reactions, charge recombination with a half-time of several seconds is observed. In the absence of Q_B, however, recombination of the separated charges between Q_A and P proceeds with a half-time of approximately 60–100 ms.

† Part of this work was supported by grants from the Deutsche Forschungsgemeinschaft to W.M. and from the European Communities (SC1000335) to W.M. and J.B. D.T. acknowledges support from NATO/NSERC for a postdoctoral fellowship. W.M. gratefully acknowledges a Heisenberg fellowship from the Deutsche Forschungsgemeinschaft.

* To whom correspondence should be addressed.

‡ Institut für Biophysik und Strahlenbiologie der Universität Freiburg.

§ CEN Saclay.

‖ Present address: Connaught Laboratories Ltd., Willowdale, Ontario, Canada.

[1] Abbreviations: Q_A and Q_B, primary and secondary quinone electron acceptors; P, primary electron donor; BChl, bacteriochlorophyll; RC, reaction center; IR, infrared; FTIR, Fourier transform infrared; UQ-10, ubiquinone-10.

0006-2960/92/0431-5799$03.00/0

The efficiency, speed, and specificity of primary photosynthetic electron transfer rely on the arrangement of the pigments in the protein scaffold. The protein, in addition, provides specific bonding and interactions for the redox cofactors, thus modulating their spectral and redox properties. The X-ray structures are an averaged static picture of the quiescent state of the RC which suggests specific interactions of the pigments and the quinones with amino acid side chains in their binding pockets (Michel et al., 1986; Allen et al., 1988; Deisenhofer & Michel, 1989; El-Kabbani et al., 1991). Spectroscopic techniques are much better suited to provide information on the dynamic processes of charge separation, stabilization, and strategic involvement of amino acids in the cofactor environment.

Optical spectroscopic techniques assess primarily the electronic states of the conjugated systems of the pigment molecules, and consequently, only little information on the binding properties and interactions of the pigments is obtained. In contrast, IR spectroscopy, which is not selective to the conjugated system of chromophores, is also advantageous for probing the properties of the protein partner. As a prize to be paid for this nonselectivity, any IR investigation of pigment protein complexes has to cope with the difficulty of the large background absorption by water, protein, and lipid. In previous work, molecular changes concomitant with primary electron transfer in bacterial and plant photosynthetic RC have been characterized by several research groups using steady-state Fourier transform infrared (FTIR) spectroscopy (Mäntele et al., 1985, 1990b; Nabedryk et al., 1986, 1990a–c; Hayashi et al., 1986; Tavitian et al., 1986; Gerwert et al., 1988; Buchanan et al., 1990, 1992; Berthomieu et al., 1990; Breton et al., 1991a,b). In these investigations, FTIR difference spectra of stable or quasi-stationary states of the RC were obtained, with a level of sensitivity high enough to detect alteration of single molecular bonds in large pigment protein complexes.

In many cases, however, reaction products cannot be stabilized, and real time resolution is desirable in order to determine sequence, rate constants, or thermodynamic parameters of a reaction. Rapid-scan FTIR spectroscopy (Braiman & Rothschild, 1988) gives access to vibrational spectroscopic information in the time range of some tens of milliseconds. This approach has been successfully applied to obtain the contribution of the quinones and their amino acid partners on the basis of the different recombination lifetimes of the photoinduced intermediates, 60–100 ms for $P^+Q_A^- \rightarrow PQ_A$ and 1–2 s for $P^+Q_AQ_B^- \rightarrow PQ_AQ_B$ (Thibodeau et al., 1990a,b).

The processes of charge stabilization on the primary and secondary electron acceptors Q_A and Q_B, as well as reactions of proton uptake upon semiquinone and dianion formation, proceed in the submicrosecond-to-millisecond domain (Wraight, 1979; Paddock et al., 1989). FTIR spectroscopy, in this time domain, can only be performed by stroboscope (Braiman et al., 1991) or step-scan (Uhmann et al., 1991) techniques. Both techniques rely on a large number of repetitive flashes applied to one sample. On the other hand, for the millisecond-to-microsecond time domain, single-wavelength IR techniques can be also applied. In earlier work, a modified dispersive IR photometer was used to record time-resolved IR absorbance changes from several photobiological systems (Siebert et al., 1980; Mäntele et al., 1982). This single-wavelength technique, however, was limited by the low sensitivity consequent to the low intensity emitted from the thermal sources of radiation used. With the advent of tunable diode lasers for the mid-IR spectral range, an optimal source of radiation has become available. In previous reports (Hienerwadel et al., 1989; Mäntele et al., 1990a), we have described a kinetic photometer based on tunable mid-IR diode lasers and its application to the study of light-induced electron transfer in RC. This system is characterized by its wide range of accessible time resolution spanning from 500 ns to several seconds. Therefore, this IR diode laser system is particularly well suited to follow electron transfer from Q_A to Q_B (ca. 120 μs) and changes of protonation state in the RC (millisecond) as well as the processes of charge recombination (millisecond or second). Here, we use this approach for the identification of vibrational absorption bands of Q_A, Q_A^- and Q_B, Q_B^- and their protein host sites. The mode frequencies of the quinones can be interpreted in terms of the nature of bonding and interaction. The time evolution of protein modes yields information on the intramolecular processes of charge stabilization.

Materials and Methods

Sample Preparation. Rb. sphaeroides R-26 RC were prepared according to Okamura et al. (1975). The secondary electron acceptor quinone Q_B was reconstituted by adding UQ-10 in excess according to Wraight (1977). The solubilized RC were then concentrated by ultrafiltration (Centricon-100, Amicon/Witten) in 20 mM Tris-HCl, pH 7.5, to a final concentration of about 0.5 mM. Approximately 5 μL of this solution was then spread on a CaF_2 window and placed under a light flow of dry N_2 to reduce the water content. The water to protein ratio was found optimal when the absorbance at 1650 cm^{-1} (amide I and water absorption) was about twice the absorbance at 1550 cm^{-1} (amide II). The CaF_2 window (20-mm diameter total) had an optically clear area of 10-mm diameter serving as the sample area. Around this spot, a grove of 0.2-mm depth and 2-mm width was ground. The outer ring of the CaF_2 window was covered with a thin layer of silicone grease. A second CaF_2 window without a grove was then pressed on top to give a cuvette of 5–15-μm path length. This thin-layer cuvette avoids the capillary action of a spacer and provides a well-sealed sample volume of only approximately 1-μL volume with a water content stable over several days. The sample thickness (estimated by monitoring the strongest absorption band at around 1650 cm^{-1}) was further adjusted to approximately 10 μm by varying the pressure onto the windows. For all measurements, this thin-layer cuvette was thermostated at 4 °C.

Time-Resolved IR Vibrational Spectroscopy. The kinetic photometer used for the detection of small light-induced IR transmittance changes has been described previously (Hienerwadel et al., 1989; Mäntele et al., 1990a). Using two continuously tunable lead salt diode lasers to generate IR-monitoring light in the 1780–1430-cm^{-1} range, single-flash-induced absorbance changes as low as 10^{-4} can be monitored. The measuring light can be directed through a monochromator (Jobin-Yvon H25, 125 line/mm grating) for wavelength calibration and elimination of laser side modes. Alternatively, the monochromator can be bypassed in order to get a higher measuring light intensity. The probe beam is then focused onto a sample spot of approximately 1-mm diameter. The transmitted light is detected by a sensitive HgCdTe IR detector (Judson Infrared, Montgomeryville, PA) which is protected from visible light by an antireflective coated Ge window. The amplified signal is recorded by a computer-controlled transient recorder (Nicolet Model 2090-3A with 8-bit, 20-ns ADC). The time resolution is limited by the detector rise time to about 500 ns. The stability of the setup allows the recording of small absorbance changes over a period of several seconds. The actinic flash at 590 nm (up to 10 mJ, 15 ns) was produced

by a dye laser (Lambda Physics DL 1000) pumped by an excimer laser (Lambda Physics EMG 53).

In order to obtain the highest instrument sensitivity to record IR absorbance changes of single bonds in a large protein complex like the RC, the monochromator bypass mode was typically used for kinetic measurements. Thus, frequencies given are those of either single laser modes of the monitoring light with a bandwidth of 10^{-3}–10^{-4} cm^{-1} or multimodes containing a main mode and one or two side modes 3–6 cm^{-1} apart from the main-mode frequency, but with an integrated intensity less than 50% of the main mode.

Time-resolved measurements in the near-IR were performed at 960 nm with a setup composed of an intense near-IR LED point source, a 960-nm band-pass filter, and a silicon diode detector in order to determine the degree of occupancy of the Q_B site in the RC samples. At this wavelength, flash-induced charge separation and recombination can be monitored by following the absorbance signal of the radical cation of the primary electron donor P^+ (Parson & Ke, 1982). Both the near-IR (960 nm) and the diode-laser mid-IR (1780–1430 cm^{-1}) kinetic photometers were designed to allow the correlation of their respective kinetic parameters for light-induced absorbance changes. The same sample spot size and position were used for both measurements, and care was taken to provide identical conditions of flash excitation. The rise time of the silicon diode detector and preamplifier was ca. 500 ns. Signal processing was performed as with the kinetic IR experiments. Thus, kinetic parameters of signals related to electronic levels of P^+/P and to changes of vibrational modes can be directly compared.

Signal Processing and Data Analysis. The amount of RC containing the secondary electron acceptor quinone Q_B was determined by a fit of the kinetic data obtained at 960 nm to a sum of two exponentials, $\alpha \exp[-k(Q_A)t] + \beta \exp[-k(Q_B)t]$. The reaction constants thus obtained [$k(Q_A)$ and $k(Q_B)$] yield the well-separated components arising from Q_A- and Q_B-containing RC. Upon normalization ($\alpha + \beta = 1$), the fraction of RC with functional secondary quinone is obtained. The same fit and normalization procedure was applied to the IR signals. The kinetic parameters of the signal at 960 nm are only due to the decay of P^+ absorbance. However, in the mid-IR region additional signals due to quinone reduction may overlap with those of P^+/P dependent on the wavelength of the IR probing beam. In this case, the time course of the IR absorbance change will deviate from that measured at 960 nm.

Let us first consider the simple time course of signals from pure modes of Q_A and of Q_B without any interference of a mode arising from the primary donor. A signal from a pure Q_A mode is characterized by a sharp absorbance decrease, which would not be resolved since the time resolution necessary to follow the disappearance of Q_A or formation of Q_A^- (200 ps) is still out of reach for the present setup. If Q_B is present, the absorbance of Q_A will be restored with 120-μs half-time, and no absorbance difference will be observed at longer time scales. If Q_B is absent, however, the absorbance of Q_A will be restored with 60–100-ms half-time. A signal from a pure Q_B mode is characterized by a decrease of absorbance with 120-μs half-time, which is restored with a half-time of several seconds. Signals from pure modes of the reduced quinone (Q_A^- or Q_B^-) follow the same time course but with an inverted sign with respect to the neutral quinone.

In the presence of a significant amount of Q_B, signals from the acceptor side of the RC (either Q_A, Q_A^-, Q_B, Q_B^-, or their respective host sites) can be identified by the observation of a 120-μs transient component. This can be verified by analyzing samples with different amounts of Q_B. The amplitude of the transient signal should then be proportional to the concentration of functional Q_B in the sample; this test is demonstrated below (see Figure 4). In addition, signals from the acceptor side can be identified by careful analysis of the charge recombination in the millisecond-to-second domain for samples containing intermediate amounts (around 50%) of Q_B: the ratio of the slow and fast components from Q_A and Q_B recombination should be changed with respect to the pure P^+ signal at 960 nm. An example of this is further demonstrated in Figure 5.

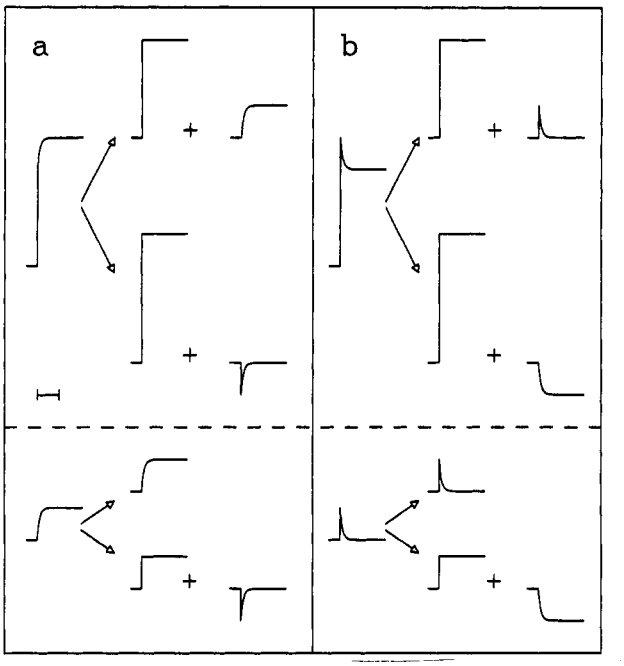

FIGURE 1: Schematic representation of composite kinetic IR signals from the P^+/P, Q_A^-/Q_A, and Q_B^-/Q_B transitions expected in the IR spectral range. (a) Upper: a sharp absorbance increase with a positive 120-μs transient can be composed either of a signal from P^+ and a positive transient from the formation of Q_B^- or of a stronger signal from P^+/P and a negative signal from a Q_A band. Lower: a positive transient may either correspond to a pure Q_B^- mode or be composed of a P^+ signal and an equally strong signal from Q_A. (b) Upper: a sharp absorbance increase with a superimposed negative 120-μs transient can be composed either of a P^+ and a Q_A^- signal or of a signal from P^+ and a signal from Q_B. Lower: a sharp rising signal which decays to zero with a 120-μs time constant may either correspond to a pure Q_A^- mode or be composed of a P^+ signal and an equally strong signal from Q_B.

However, complex overlaps from P^+/P, Q_A^-/Q_A, and Q_B^-/Q_B also have to be considered, making unambiguous assignment of any signal impracticable, as demonstrated below. In the scheme of Figure 1 some composite signals from modes of P^+/P, Q_A^-/Q_A, and Q_B^-/Q_B are summarized. According to Figure 1a, a positive signal consisting of a sharp-rising component (step signal) and a positive 120-μs transient signal can be obtained from a P/P^+ signal and a positive transient 120-μs signal upon formation of Q_B^- but also from a (larger) P^+/P signal and a negative signal from Q_A, diagnostic for the reaction $Q_A \rightarrow Q_A^- \rightarrow Q_A$. In the absence of a step signal (Figure 1a, lower part), a 120-μs transient, apart from being attributed to "pure" Q_B^-, might still be composed from a small positive P^+/P component and a signal from Q_A of identical initial amplitude. In a similar way, a positive sharp-rising component with a negative 120-μs transient (Figure 1b, upper part) is either a positive Q_A^- signal or a negative Q_B signal superimposed onto P^+/P step signals of different amplitudes. As illustrated in Figure 1b (lower part), a sharp-rising signal decaying back to zero with 120-μs half-time, apart from being

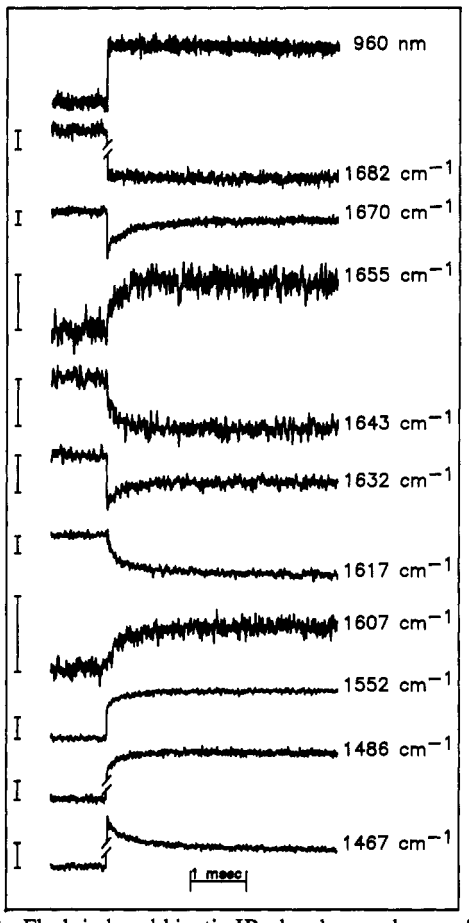

FIGURE 2: Flash-induced kinetic IR absorbance changes from *Rb. sphaeroides* RC at 4 °C. Signals are shown at the same time scale (see bar) but at different absorbance scales (bar length corresponds to 2×10^{-4} absorbance unit). For the signals at 1467, 1486, and 1682 cm^{-1}, the amplitude of the sharp rise corresponds to 1.1×10^{-3} absorbance unit and is shown further compressed with respect to the slower rise. Excitation: 595 nm, 5 mJ, 15 ns. Up to 300 flashes were averaged for each signal.

attributed to Q_A^-, might still be composed from a small P^+/P signal and a negative Q_B component of identical amplitude. Thus, regardless of the initial amplitude of the superimposed signal, an increasing transient signal (120-μs half-time) corresponds to either the formation of Q_B^- or the restoring of Q_A. On the other hand, a decreasing signal corresponds to either the disappearance of the state Q_A^- or the restoring of Q_B. Signals arising from modes of either Q_A^- or Q_B and signals arising from modes of either Q_A or Q_B^- cannot be distinguished by the kinetic analysis alone, since either of the two couples can provide a rising or decreasing 120-μs transient. However, the sign of the 120-μs transient can be obtained by using additional information from model compound spectra on the approximate region of Q or Q^- modes (Bauscher et al., 1990; Bauscher, 1991) and from light-induced or electrochemically induced FTIR difference spectra on RC (Mäntele et al., 1990b; Thibodeau et al., 1990a,b; Breton et al., 1991a,b; Bauscher, 1991).

Results and Discussion

Figure 2 shows kinetic signals at discrete wavenumbers in the 1700–1450-cm^{-1} spectral range obtained with a *Rb. sphaeroides* RC sample reconstituted with Q_B. For comparison, a kinetic signal recorded at 960 nm is also shown on the same time scale. The amount of RC decaying with a half-time of around 1.5 s, indicating that Q_B is present and functional, was estimated to about 90% of the total amount of RC as determined by the kinetic analysis of the signal at

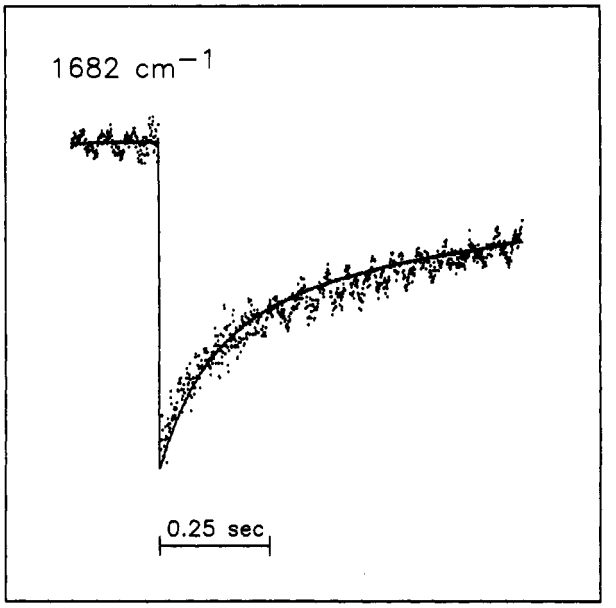

FIGURE 3: Flash-induced kinetic IR signal at 1682 cm^{-1} obtained by averaging 20 flashes. The smooth line through the noisy trace corresponds to the kinetic signal at 960 nm representing the formation and decay of $(BChl)_2^+$ (scaled to the same amplitude and inverted). Excitation was as in Figure 2.

960 nm. At the time scale shown (5 μs/data point; 1024 data points), many of the traces exhibit a rapid (within the instrument rise time of ca. 500 ns) flash-induced absorbance change without significant decay during the total recording time. Since the signal amplitudes vary considerably, the traces are shown on different scales, with a bar indicating the size of a 2×10^{-4} absorbance unit. The signals at 1682, 1486, and 1467 cm^{-1} are shown in a compressed scale.

In addition to these sharp-rising signals, transient absorption changes are found at many wavenumbers with half-times in the range of 120 ± 50 μs. The largest absorbance changes arising from these time-resolved transient signals are approximately 8 times smaller than the strongest sharp-rising signal. Both signal types appear together in most cases, but several wavelengths have been characterized where either the step signal (for example at 1682 cm^{-1}) or the 120-μs transient component (for example at 1607, 1617, 1643, 1655 cm^{-1}) predominantly appears. In addition to the traces shown, many other signals have been recorded to determine band shapes and zero crossovers.

We attribute the sharp-rising signals to the process of immediate charge separation between the primary electron donor P and the primary electron acceptor Q_A ($PQ_AQ_B \rightarrow P^+Q_A^-Q_B$), which takes place in about 200 ps (Parson & Ke, 1982). The 120-μs component is attributed to the transfer of the electron from the primary to the secondary quinone acceptor, $P^+Q_A^-Q_B \rightarrow P^+Q_AQ_B^-$ (Wraight, 1979). Indeed, difference spectra obtained from individual signals in the 1700–1760-cm^{-1} range (Hienerwadel et al., 1989) or around 1680 cm^{-1} (data not shown) closely correspond to rapid-scan FTIR $P^+Q_A^-/PQ_A$ and $P^+Q_B^-/PQ_B$ difference spectra (Thibodeau et al., 1990a,b).

At 1682 cm^{-1} (see Figure 2) and 1703–1720 cm^{-1} (Hienerwadel et al., 1989), predominantly sharp-rising signals are observed, regardless of the Q_B content of the sample. Figure 3 shows a kinetic signal at 1682 cm^{-1} together with the corresponding absorbance change at 960 nm. Both signals decay on time scale of seconds; an analysis yields identical kinetic parameters. On the basis of redox-induced IR difference spectra of isolated BChls (Mäntele et al., 1988; Leonhard et al., 1989), a 1682-cm^{-1} band in light-induced P^+Q^- FTIR

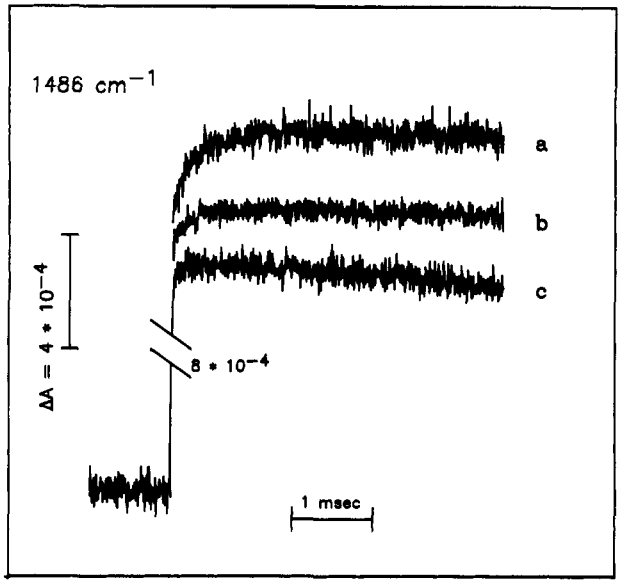

FIGURE 4: IR signal at 1486 cm^{-1} for RC containing different amounts of Q_B (a, >90%; b, ca. 50%, c, <10%) as determined by the analysis of the kinetic parameters of charge recombination at 960 nm. The sharp rise immediately after the flash is shown compressed with respect to the slow component.

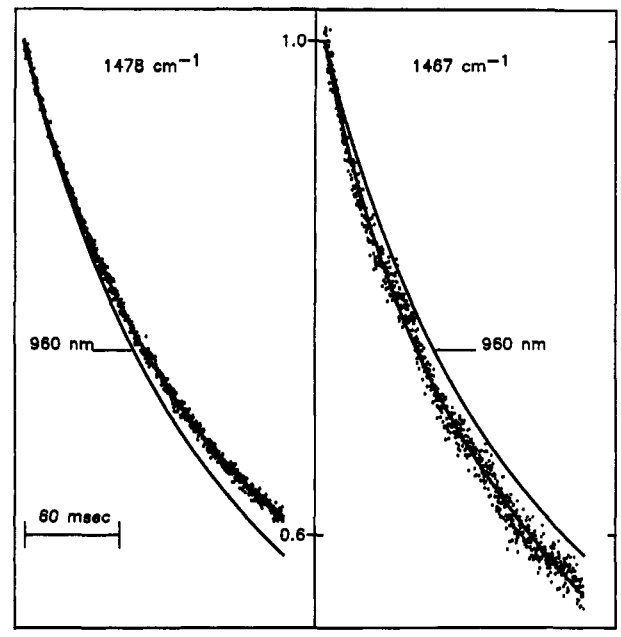

FIGURE 5: Comparison of IR and NIR (960 nm) signal decay at 1478 and 1467 cm^{-1}. The solid lines represent a two-exponential fit to the IR and NIR signals. Left: the signal at 1478 cm^{-1} decays more slowly than the normalized signal at 960 nm. Right: the signal at 1467 cm^{-1} decays more rapidly than the normalized signal at 960 nm. For details see text.

difference spectra has been assigned to the 9-keto C=O vibration of the primary electron donor BChl(s) in the neutral state. Correspondingly, the 1702–1716-cm^1 signals in these FTIR difference spectra have been attributed to the appearance and decay of the 9-keto C=O vibration of the radical cation of the primary electron donor. In photochemically induced Q_A^-/Q_A and Q_B^-/Q_B (Breton et al., 1991a,b; Bauscher, 1991) and electrochemically induced Q_A^-/Q_A (Mäntele et al., 1990b; Bauscher, 1991) FTIR difference spectra, negative signals are observed around 1690 cm^{-1} (Q_A) and at 1685 cm^{-1} (Q_B). Superposition of both quinones signals, at equal contribution, might cancel the 120-μs transient component at 1682 cm^{-1}. However, the contributions from P^+/P are considerably stronger than those of Q_A in this region (Mäntele et al., 1990b; Breton, 1991a; Bauscher, 1991). We thus attribute the IR signals at 1682 and 1702–1716 cm^{-1} (Hienerwadel et al., 1989) predominantly to changes of vibrational modes of the primary electron donor.

A transient signal exhibiting 120-μs rise (or decay) time is expected to arise from changes of vibrational modes of the RC acceptor side, i.e., either from Q_A or Q_B, including the amino acids forming their binding pockets. In order to test this hypothesis, RC with different contents of the secondary acceptor Q_B were analyzed. Figure 4 shows the time-resolved IR signals at 1486 cm^{-1} for RC samples with high (>90%), intermediate (ca. 50%), and low (<10%) content of Q_B, normalized on the signal amplitude at 960 nm. While the amplitude of the sharp-rising signal (shown on a compressed scale) is constant for all three RC samples, the transient signal is proportional to the content of Q_B calculated from the analysis of charge recombination parameters observed at 960 nm.

As discussed above, an increasing 120-μs transient signal corresponds to either the formation of Q_B^- or the restoring of Q_A, and a decreasing signal corresponds to either the disappearance of the state Q_A^- or the restoring of Q_B. On this basis, we attribute the signals at 1643, 1617, and 1467 cm^{-1} to either Q_A^- or Q_B (and their respective host site), because these signals exhibit decreasing transient components. Increasing transient signals are found at 1486, 1552, 1607, 1632, 1655, and 1670 cm^{-1} and attributed to modes of either Q_A or Q_B^- (and their respective host site). These transients remarkably agree both in frequency and in amplitude with $Q_A^-Q_B/Q_AQ_B^-$ double difference spectra obtained by rapid-scan FTIR spectroscopy (Thibodeau et al., 1990a,b). This technique made use of the well-separated decay times from the states $P^+Q_A^-Q_B$ and $P^+Q_AQ_B^-$ to obtain a $Q_A^-Q_B/Q_AQ_B^-$ double difference spectrum without contributions from the state P^+/P. In contrast to this method, the measurements presented here are based on the *direct* observation of the vibrational modes changing upon forward charge transfer between Q_A^- and Q_B.

The fact that observation of forward charge transfer and decay of the charge-separated states can lead to the same attribution of vibrational modes of the quinones is further illustrated by analyzing the back-reaction kinetics. As an example Figure 5 shows the signals at 1478 and 1467 cm^{-1} after normalization of the amplitude as described above, together with the 960-nm signal. The normalized IR signal at 1478 cm^{-1} decays more slowly than the normalized 960-nm signal, while the IR signal at 1467 cm^{-1} decays more rapidly. We thus concude that the signal at 1478 cm^{-1} arises from a mode of either Q_A or Q_B^-, whereas that at 1467 cm^{-1} arises from either Q_A^- or Q_B. Both signals (the one at 1467 cm^{-1} is shown in Figure 2) exhibit a significant contribution from the 120-μs transient. Thus, analyzing the 120-μs transients and the back-reaction kinetics leads to the same conclusions.

Reduction of Q_A and Q_B by electron transfer should give rise to strong difference bands of the C=O and the C=C modes. FTIR difference spectra of semiquinone anion, dianion, and hydroquinone formation have been obtained by electrochemical reduction of model quinones (Bauscher et al., 1990; Bauscher, 1991). The two C=O modes of neutral 2,3-dimethoxy-5-methyl-1,4-benzoquinone were found at 1659 cm^{-1} (deuterated methanol) and at 1660 cm^{-1} (deuterated acetonitrile), respectively. The C=O modes of 2,3-dimethoxy-5-methyl-6-isoprenyl-1,4-benzoquinone (UQ-1) are found at 1650 cm^{-1} (methanol) and at 1648 cm^{-1} (acetonitrile), respectively. The carbonyl frequency in model compounds thus depends more on the presence of substituents than on the ability of the solvent to form hydrogen bonds and (or) on the

influence of the polarity of the solvent on the quinone ring system (Bauscher, 1991, and references therein). Ubiquinone-10 in the polar, nonprotic solvent tetrahydrofuran shows two C=O modes at 1650 and 1666 cm^{-1} (Bauscher, 1991). The C=C modes of ubiquinones were found between 1606 and 1612 cm^{-1} (Bauscher et al., 1990; Bauscher, 1991). The electrochemically generated quinone model difference spectra show a disappearance of the strong C=O and of the C=C mode(s). The C—O and C—C modes of the semiquinone anion from ubiquinones are clearly separated in frequency from the C=O and the C=C modes of the neutral form and were found between ca. 1490 and ca. 1465 cm^{-1}, respectively (Bauscher, 1991).

The signal at 1670 cm^{-1} (Figure 2) shows a rapid decrease of the absorbance, which is almost fully restored with the kinetic parameters of the $Q_A \rightarrow Q_B$ electron transfer. It appears reasonable to attribute this signal to a mode of Q_A and/or to changes in its binding pocket. One could argue that this transient signal arises from an overlap of an absorbance band of the neutral state of the primary electron donor (giving rise to a negative signal) and from a signal of the Q_B^- state (giving rise to a positive 120-μs transient). In this case, only modes from the protein host site of Q_B^- should be taken into consideration, since no absorbance of the quinone anion itself is observed in this frequency range (Bauscher et al., 1990; Bauscher, 1991). However, the electrochemically generated P^+/P difference spectrum (Mäntele et al., 1990b) does not exhibit a strong band in this region. On the other hand, the strongest negative signal in Q_A^-/Q_A difference spectra (Mäntele et al., 1990b; Breton et al., 1991a; Bauscher, 1991) is observed at 1668–1671 cm^{-1}. These arguments support an assignment of the transient (120-μs) signal at 1670 cm^{-1} to a mode from the Q_A state. A possibility would be to assign the band at 1670 cm^{-1} to the C=O mode of the neutral Q_A. However, $P^+Q_A^-/PQ_A$ difference spectra obtained with chemically modified or isotopically labeled (^{13}C, ^{18}O) quinones did not show evidence for shifts of bands in this spectral region (Bagley et al., 1990). Furthermore, time-resolved FTIR experiments with ^{13}C isotope labeling of Q_A and Q_B indicate that the 1670-cm^{-1} band remains at the same position (Thibodeau et al., 1990a,b).

The same time course is observed for the signal at 1632 cm^{-1}, although a stronger negative step-like signal is superimposed. One might consider a composite signal from P (negative step signal) and from Q_B^- (positive 120-μs transient). Since light-induced Q_B^-/Q_B difference spectra (Breton et al., 1991b; Bauscher, 1991) exhibit C=O signals in this frequency range, this explanation seems less likely. It appears possible that the stronger negative step-like signal is caused by a significant contribution from P as attested by the electrochemically induced pure P^+/P difference spectra (Mäntele et al., 1990b). We thus propose that the transient signal at 1632 cm^{-1} can be attributed to Q_A, in line with the assignment of a negative band at 1632–1633 cm^{-1} in Q_A^-/Q_A difference spectra (Mäntele et al., 1990b; Breton et al., 1991a; Bauscher, 1991). The possibility that this band might represent the disappearing C=O mode of Q_A has been discussed (Mäntele et al., 1990b; Thibodeau et al., 1990a,b). However, this rather low value for the C=O frequency is difficult to justify regarding the Q_A protein environment, which is of low polarity and contains a number of aromatic amino acid residues (Allen et al., 1988; El-Kabbani et al., 1991).

The signal at 1655 cm^{-1} corresponds to an absorbance increase upon Q_B reduction; it excludes it from being a candidate for the Q_B C=O. Assignment to the amide I mode of one of the amino acids forming the Q_B pocket is therefore considered. An alternative, though more complicated interpretation would be a negative transient signal arising from the Q_A binding pocket, with the additional superposition of a positive signal from the primary donor. However, no positive band in the P^+/P difference spectrum is observed around 1655 cm^{-1} (Mäntele et al., 1990b). In addition, Q_B^-/Q_B difference spectra exhibit small positive contributions around 1655 cm^{-1} (Breton et al., 1991b; Bauscher, 1991). Thus, attribution of the signal at 1655 cm^{-1} to one of the amino acids forming the Q_B binding pocket is more likely. On the other hand, Q_A^-/Q_A difference spectra obtained photochemically (Breton et al., 1991a) or electrochemically (Mäntele et al., 1990b) show negative bands at 1654 and 1651 cm^{-1}, respectively, which could be related to the negative band at 1650 cm^{-1} found in the $P^+Q_A^-/PQ_A$ experiments (Nabedryk et al., 1990b; Bagley et al., 1990). This band was interpreted in terms of a conformational change near Q_A upon reduction of Q_A. Since no laser diode monomodes were available around 1650 cm^{-1}, a clear analysis of the signal profile was not possible by time-resolved spectroscopy. We do not, however, exclude the possibility that the time-resolved measurements presented here, which essentially monitor forward electron transfer and the unrelaxed protein, differ from the steady-state FTIR difference spectra referred to above. In addition, the time-resolved IR data monitor Q_A reduction in the presence of functionally active Q_B, in contrast to previous investigations performed on RC either lacking Q_B or with blocked $Q_A^-Q_B \rightarrow Q_AQ_B^-$ electron transfer.

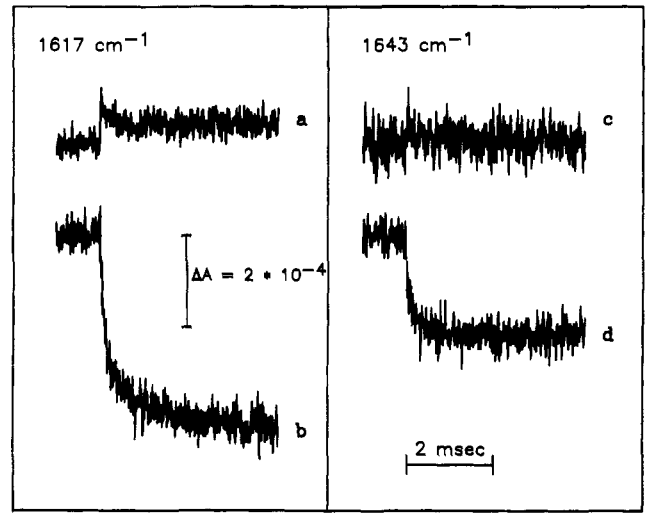

FIGURE 6: IR signals at 1617 and 1643 cm^{-1} without (a, c) and with (b, d) the secondary electron acceptor Q_B present. Excitation was as in Figure 2. Note the slow ~1-ms component in addition to the 120-μs component in (b).

The signals at 1643 and 1617 cm^{-1} exhibit a 120-μs component without a significant step signal. As seen in Figure 6a,c almost no signals are observed at 1643 and 1617 cm^{-1} in the absence of Q_B. The lack of a sharp-rising component implies either that these frequencies represent isosbestic points for both P^+/P and Q_A^-/Q_A or that both signals almost precisely cancel each other. On the other hand, the transient signal observed in the presence of Q_B implies that a mode of either Q_A^- or Q_B is predominantly present at these wavenumbers. In the first case of isosbestic points for P^+/P and Q_A^-/Q_A at 1643 and at 1617 cm^{-1}, the transient signals are due to modes of Q_B or its protein host site. In the second case of an almost complete cancellation of P^+/P and Q_A^-/Q_A signals (which might be of unknown amplitude) in the absence of Q_B, the transient signals in the presence of Q_B might arise predominantly from a mode of Q_A.

In order to resolve this ambiguity, we have compared these signals with Q_A^-/Q_A difference spectra obtained electrochemically (Mäntele et al., 1990b; Bauscher, 1991) or photochemically (Breton et al., 1991a; Bauscher, 1991). These difference spectra do not exhibit strong difference bands at these frequencies, nor does the electrochemically induced P^+/P difference spectrum (Mäntele et al., 1990b). However, photochemically generated Q_B^-/Q_B difference spectra recently obtained by Breton et al. (1991b) show Q_B signals at these frequencies. We thus conclude that the 120-μs transient signals observed at 1643 and at 1617 cm^{-1} predominantly arise from modes of Q_B and its host site and represent the dynamic processes upon Q_B reduction. We would like to emphasize that the generally good agreement of band amplitudes and positions between the steady-state difference spectra and the signals presented in this work indicates that the majority of the relaxation processes occur within the 120-μs kinetics of Q_B reduction.

The Q_B signal at 1643 cm^{-1} is a candidate for the C=O mode of Q_B as also proposed by Breton et al. (1991b), although its frequency would be significantly lowered compared to the C=O mode observed from isolated ubiquinones (1650–1666 cm^{-1}) (Bauscher et al., 1990; Bauscher, 1991, and references therein). After all, it is difficult to predict from the C=O frequencies of isolated quinones in a homogeneous solvent of a given polarity or proton activity the mode frequencies of a quinone, bound in a binding pocket of inhomogeneous polarity. In addition to bonding of the carbonyls to appropriate groups of the protein, the influence of π–π interactions with neighboring groups in the protein appears to have a relevant influence on the C=C and C=O modes. Slifkin and Walmsley (1970) have analyzed the vibrational spectra of quinhydrone-type complexes and ascribed the lowering of the C=O frequencies predominantly to π–π interactions. In the Q_B binding site, H-bonding of the Q_B to His 190 and Ser 223 side chains (Allen et al., 1988; El-Kabbani et al., 1991) might account for the lowering of the C=O frequency.

In the 1580–1520-cm^{-1} region, several sharp-rising signals are found, which we attribute to $P^+Q_A^-$ formation. An example of a signal at 1552 cm^{-1} showing a significant contribution from $Q_A^-Q_B \rightarrow Q_AQ_B^-$ electron transfer is given in Figure 2. The amplitude of the signals between 1580 and 1520 cm^{-1} as a function of wavelength for this region correlates with that of the P^+ and the Q^- formation as obtained for electrochemically and light-induced P^+ and Q^- difference spectra (Mäntele et al., 1990b; Thibodeau et al., 1990b; Breton et al., 1991a,b). The bands are within the expected range for aromatic C=C vibrations (Chirgadze et al., 1975; Venyaminov & Kalnin, 1990). It has been proposed that these signals are due to perturbations of the aromatic residues close to Q_A upon reduction (Mäntele et al., 1990b; Thibodeau et al., 1990a,b; Breton et al., 1991a,b). Possible candidates are Trp M252, Trp M268, and/or Phe M258 and M251.

The 1486-, 1478-, and 1467-cm^{-1} signals are composed of both a positive sharp-rising component from the P^+/P transition and a 120-μs transient (Figures 2 and 4). In fact, electrochemically generated P^+/P difference spectra show a positive band structure between ca. 1440 and ca. 1495 cm^{-1} (Mäntele et al., 1990b). The existence of semiquinone anion bands in this frequency range has been demonstrated from model quinone compound studies (Bauscher et al., 1990; Bauscher, 1991). Time-resolved FTIR double difference spectra (Thibodeau et al., 1990a,b) show a complex negative band structure at 1493 and 1480 cm^{-1} and a positive band at 1460 cm^{-1} that have been assigned to C—C and/or C—O

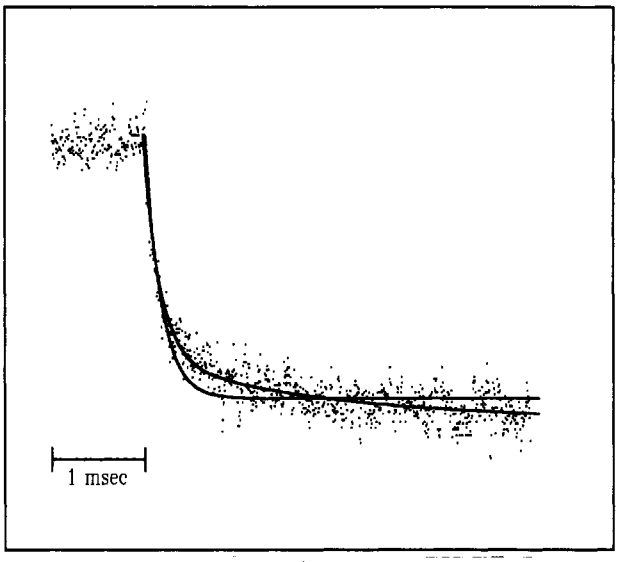

FIGURE 7: IR signal at 1617 cm^{-1} (same as in Figure 6b). The two solid lines represent fits to the data with a single-exponential function (120-μs, 100% amplitude) and with two exponentials (120 μs, 60%; 1.2 ms, 40% amplitude).

vibrations of Q_B^- (negative bands) and Q_A^- (positive band), respectively. Indeed, time-resolved FTIR experiments with ^{13}C-isotope-labeled quinones revealed shifts of these bands. The different absorption bands for the two semiquinone anions (Q_A^-, Q_B^-) are confirmed by the kinetic signals presented here and lead us to assign the 1486- and 1478-cm^{-1} signals to modes of Q_B^- and the 1467-cm^{-1} signal to a mode of Q_A^-. These assignments also agree with bands of Q_A^- and Q_B^- found in Mäntele et al. (1990b), Bauscher et al. (1990), Bauscher (1991), and Breton et al. (1991a,b).

Among the signals arising from Q_B^- formation, the one at 1617 cm^{-1} markedly differs, in that the time course of the signal amplitude (Figure 6b) cannot be approximated with a single 120-μs component alone. The arguments used to attribute the 120-μs transient signal to a mode of Q_B have been discussed above. It might be attributed to the C=C mode of Q_B, as has been proposed recently from light-induced Q_B^-/Q_B difference spectra (Breton et al., 1991b). An additional, much slower kinetic component with a half-time of slightly above 1 ms (hereafter termed 1-ms component) is observed in the presence of Q_B (Figure 6b), which accounts for approximately 40% of the total signal amplitude. While a single exponential fails to describe the time course of the absorption, a two-exponential fit yields a slower reaction with ca. 1.2-ms half-time (Figure 7) in addition to a fast component whose half-time was kept constant at 120 μs for the fit procedure. Attempts to describe the time course of this signal with a single-exponential function yielded half-times of 250–300 μs without a satisfactory fit.

No chromophore signal exhibits this reaction half-time upon RC single-flash turnover. However, acid–base groups from amino acids have been characterized which undergo pK shifts and protonation changes upon Q_B^- formation (Wraight, 1979; Marôti & Wraight, 1988; McPherson et al., 1988; Brzezinski et al., 1991), leading to a net H^+ uptake of about one H^+ per electron transferred by the RC. The rate of proton uptake was found similar to or slightly lower than that of Q_B reduction [see Figure 3 in Wraight (1979)].

Although the 1-ms component observed at 1617 cm^{-1} is considerably slower than the half-time of 250 μs for H^+ uptake at pH 7.5 (Wraight, 1979), we are tempted to ascribe it to (one of) the acid–base group(s) that are involved in proton

binding upon reduction of Q_B. Since the 1617-cm^{-1} signal only appears in the presence of Q_B, we exclude a contribution arising from protonation upon Q_A^- formation. The absence of an indicator dye and the comparatively low amount of bulk water in the highly concentrated samples used in our experiments might well account for the difference in the rates observed.

According to the vibration frequency, this signal might be assigned to the strong antisymmetric C—O mode of a carboxylate group (Bellamy, 1975), which upon reduction of Q_B shifts its pK in response to the electrostatic interaction and may be partially protonated to become a carboxyl group. As an alternative explanation for the 1-ms signal, we have considered the possibility that a small fraction of Q_B^- is accumulated in our samples upon flash excitation, even in the absence of exogenous donors. The fact that the signal at 1478 cm^{-1}, which we attribute to a mode of Q_B^-, does not exhibit this 1-ms transient makes this explanation unlikely.

A second, alternative explanation for the 1-ms component might be a biphasic electron transfer to Q_B, with a rapid phase of ca. 100–200 μs and a slow phase of ca. 1 ms, as observed by Takahashi et al. (1991). If, however, $Q_A^-Q_B \rightarrow Q_AQ_B^-$ electron transfer in our samples would proceed with heterogeneous kinetic parameters, all genuine quinone modes should reveal this biphasic reaction. As already stated above for a potential accumulation of Q_B^-, the presence of clearly "monophasic" signals from genuine Q_A and Q_B modes makes this interpretation unlikely.

A signal at 1617 cm^{-1}, instead of being caused by a pK shift and protonation (with the consequence of bleaching of the band), might alternatively arise from a change of environment for a carboxylate. This last possibility would lead to a differential feature. At the present state, we have no evidence for a possible rising 1-ms counterpart of the 1617-cm^{-1} millisecond signal in the 1600–1630-cm^{-1} wavelength range and thus conclude that a pK shift seems more likely.

The binding pocket of Q_B contains a number of ionizable amino acid residues (Allen et al., 1988; El-Kabbani et al., 1991). The carbonyls of Q_B are within H-bonding distance to Ser L223 and to His L190. In addition, Glu L212 and Asp L213 are in close contact to the quinone. Paddock et al. (1989, 1990) have proposed a model where Ser L223 and Glu L212 are involved in protonation of Q_B upon formation of the state $Q_A^-Q_B^-$. Paddock et al. (1989) have furthermore suggested that Glu L212 is responsible for the variation of the $Q_A^-Q_B \rightarrow Q_AQ_B^-$ and the $P^+Q_B^- \rightarrow PQ_B$ reaction rates at high pH and have reported an anomalously high pK_a value of 9.5 for this group. It is thus unlikely that, in our experimental conditions (pH 7.5), the 1617-cm^{-1} signal, which we tentatively attribute to protonation of a carboxylate, can arise from Glu L212.

The crucial role for Asp L213 was pointed out by Takahashi and Wraight (1990), Paddock et al. (1990, 1991), Rongey et al. (1991), and McPherson et al. (1991), in that its replacement by Asn slows down the rate of transfer of the first and the second electron to Q_B and abolishes the pH dependence of charge recombination between pH $\approx$ 4 and pH $\approx$ 7. The pK_a of Asp L213 was proposed to be approximately 4.5–5 for neutral Q_B (Takahashi & Wraight, 1990; Paddock et al., 1991), shifting to approximately 7 for Q_B^- (Paddock et al., 1991). In this view, the signal observed at 1617 cm^{-1} may be tentatively assigned to the antisymmetric C—O mode of Asp L213.

Q_B protonation from the outside of the RC may involve a proton-transfer chain as proposed, for example, for bacteriorhodopsin (Henderson et al., 1990) but also possibly tunneling processes to bridge longer distances. Whether a proton-tunneling mechnanism from the outside of the RC toward Asp L213, slower than the triggering reduction of Q_B, could account for the observed reaction rate cannot be answered yet. Furthermore, it cannot be excluded at present that a more complicated pathway of protonation exists, with even more distant groups involved, for example, in the H-polypeptide subunit. It appears consistent, however, that the protonation of Asp L213, which is normally ionized and presents an electrostatic restriction to the $Q_A^-Q_B \rightarrow Q_AQ_B^-$ electron transfer, stabilizes the state Q_B^- until a second electron is transferred.

A second, although less probable candidate for an amino acid side-chain group which is IR active in this spectral region (at somewhat higher frequencies) and is possibly involved in protonation reactions would be the NH_2^+ group of His L190, a ligand to the Q_B carbonyl (Paddock et al., 1990). In the case of a ligand to Q_B, however, one would expect identical kinetic parameters for the quinone reduction and the histidine protonation change. In addition, the sign of the signal would correspond to a deprotonation. This model appears less suitable to explain the results.

Protonation of a carboxylate group could be tracked not only by the disappearance of the antisymmetric C—O vibration but also by the disappearance of the corresponding symmetric form below 1450 cm^{-1} and by the appearance of the carboxyl C=O vibration between 1730 and 1760 cm^{-1} (Bellamy 1968, 1975). The position of this band would strongly depend on hydrogen bonding (Siebert et al., 1982). Indeed, a kinetic analysis of the carboxyl frequency range, together with the frequency range for the antisymmetric C=O vibrations, would allow tracing of the protons from the outside of the RC to the environment of Q_B^-. In preliminary experiments, we have been able to detect a weak 1-ms component around 1720–1740 cm^{-1}, superimposed on the strong signal of the 10a ester C=O vibration of the primary donor BChl upon P^+ formation. This finding supports the preliminary assignment given above. However, further experiments using RC modified by site-directed mutagenesis will be necessary to verify this hypothesis.

CONCLUSIONS

The time-resolved IR study presented here allows us to follow the dynamic processes of electron transfer and protein conformation upon reduction of the primary and secondary quinone electron acceptors in RC. Previous studies from our laboratories have investigated these reduction states under either steady state or flash illumination but have observed the relaxed state of the protein. The generally excellent agreement for most of the observed signals between steady-state measurements and the time-resolved signals presented here demonstrates that this protein relaxation is extremely fast and closely follows the electron transfer.

In the case of the primary quinone Q_A, there is no indication for protein relaxation phases, at least within the present signal-to-noise ratio. This demonstrates that, upon Q_A reduction, proteic readjustments, if any, are faster than the time resolution used here (5 μs). In the case of the secondary quinone Q_B, the millisecond signal observed at 1617 cm^{-1} (and less pronounced, at a few other frequencies) represents direct spectroscopic evidence for the relaxation of a cofactor environment in response to a change in its redox state.

At the present state of our investigations, not all of the multiple bands in difference spectra showing Q_A or Q_B reduction (Mäntele et al., 1990b; Thibodeau et al., 1990a,b; Breton et al., 1991a,b; Bauscher 1991) have been probed in detail for further "millisecond components" by this time-re-

solved technique. However, it appears reasonable to assume that the millisecond component observed at 1617 cm^{-1} represents direct evidence for a protonation change consequent to Q_B reduction. Further experiments at a series of pH values, with site-directed mutations in the Q_B site, and experiments using double-flash excitations will be necessary to trace the pathway of protons into the RC to Q_B.

ACKNOWLEDGMENTS

We thank Dr. D. A. Moss and S. Grzybek for their help with computer programs to control the kinetic photometer and the transient recorder and Dr. M. Bauscher for stimulating discussions and for providing unpublished data from his Ph.D. thesis. We are indebted to the laser technology group of the Fraunhofer Institut für Physikalische Messtechnik at Freiburg for producing and supplying the IR diode lasers.

Registry No. Aspartic acid, 56-84-8.

REFERENCES

Allen, J. P., Feher, G., Yeates, T. O., Komiya, H., & Rees, D. C. (1988) *Proc. Natl. Acad. Sci. U.S.A. 85*, 8487–8491.

Bagley, K. A., Abresch, E., Okamura, M. Y., Feher, G., Bauscher, M., Mäntele, W., Nabedryk, E., & Breton, J. (1990) in *Current Research* in *Photosynthesis* (Baltscheffsky, M., Ed.) Vol. I, pp 77–80, Kluwer Academic Publishers, Dordrecht, The Netherlands.

Bauscher, M. (1991) Ph.D. Thesis, Faculty of Chemistry, Universität Freiburg.

Bauscher, M., Nabedryk, E., Bagley, K. A., Breton, J., & Mäntele, W. (1990) *FEBS Lett. 261*, 191–195.

Bellamy, L. J. (1968) *Advances in infrared group frequencies*, Vol. 2, Chapman & Hall, London.

Bellamy, L. J. (1975) *The infrared spectra of complex molecules*, 3rd ed., Chapman & Hall, London.

Berthomieu, C., Nabedryk, E., Mäntele, W., & Breton, J. (1990) *FEBS Lett. 269*, 363–367.

Braiman, M., Ahl, P., & Rothschild, K. J. (1987) *Proc. Natl. Acad. Sci. U.S.A. 84*, 5221–5225.

Braiman, M., Bousche, O., & Rothschild, K. (1991) *Proc. Natl. Acad. Sci. U.S.A. 88*, 2388–2392.

Breton, J., Martin, J. L., Fleming, G. R., & Lambry, J. C. (1988) *Biochemistry 27*, 8276–8284.

Breton, J., Thibodeau, D. L., Berthomieu, C., Mäntele, W., Verméglio, A., & Nabedryk, E. (1991a) *FEBS Lett. 278*, 257–260.

Breton, J., Berthomieu, C., Thibodeau, D. L., & Nabedryk, E. (1991b) *FEBS Lett. 288*, 109–113.

Brzezinski, P., Paddock, M. L., Rongey, S. H., Okamura, M. Y., & Feher, G. (1991) *Biophys. J. 59*, 143a.

Buchanan, S., Michel, H., & Gerwert, K. (1990) in *Reaction Centers of Photosynthetic Bacteria* (Michel-Beyerle, M. E., Ed.) Springer Series in Biophysics, Vol. 6, pp 75–85, Springer, Berlin.

Buchanan, S., Michel, H., & Gerwert, K. (1992) *Biochemistry 31*, 1314–1322.

Chang, C.-H., El-Kabbani, O., Tiede, D., Norris, J., & Schiffer, M. (1991) *Biochemistry 30*, 5352–5360.

Chirgadze, Y. N., Fedororov, O. V., & Trushina, N. P. (1975) *Biopolymers 14*, 679–694.

Deisenhofer, J., & Michel, H. (1989) *EMBO J. 8*, 2149–2170.

El-Kabbani, O., Chang, C.-H., Tiede, D., Norris, J., & Schiffer, M. (1991) *Biochemistry 30*, 5361–5369.

Gerwert, K., Hess, B., Michel, H., & Buchanan, S. (1988) *FEBS Lett. 232*, 303–307.

Hayashi, H., Go, M., & Tasumi, M. (1986) *Chem. Lett.*, 1511–1514.

Henderson, R., Baldwin, J. M., Ceska, T. A., Zemlin, F., Beckmann, E. & Downing, K. H. (1990) *J. Mol. Biol. 213*, 899–929.

Hienerwadel, R., Kreutz, W., & Mäntele, W. (1989) in *Spectroscopy of Biological Molecules—State of the Art* (Bertoluzza, A., Fagnano, C., & Monti, P., Eds.) pp 315–316, Societa Editrice Esculapio, Bologna, Italy.

Holzapfel, W., Finkele, U., Kaiser, W., Oesterhelt, D., Scheer, H., Stilz, H. U., & Zinth, W. (1989) *Chem. Phys. Lett. 160*, 1–7.

Leonhard, M., Wollenweber, A., Berger, G., Kleo, J., Nabedryk, E., Breton, J., & Mäntele, W. (1989) in *Techniques and Developments in Photosynthesis Research* (Barber, J., & Malkin, R., Eds.) pp 115–118, Plenum Publishing Corp., New York.

Mäntele, W., Siebert, F., & Kreutz, W. (1982) *Methods Enzymol. 88*, 729–740.

Mäntele, W., Nabedryk, E., Tavitian, B. A., Kreutz, W., & Breton, J. (1985) *FEBS Lett. 187*, 227–232.

Mäntele, W., Wollenweber, A., Nabedryk, E., & Breton, J. (1988) *Proc. Natl. Acad. Sci. U.S.A. 85*, 8468–8472.

Mäntele, W., Hienerwadel, R., Lenz, F., Riedel, W. J., Grisar, R., & Tacke, M. (1990a) *Spectrosc. Int. 2*, 29–35.

Mäntele, W., Leonhard, M., Bauscher, M., Nabedryk, E., Breton, J., & Moss, D. A. (1990b) in *Reaction Centers of Photosynthetic Bacteria* (Michel-Beyerle, M. E., Ed.) Springer Series in Biophysics, Vol. 6, pp 31–44, Springer, Berlin.

Marôti, P., & Wraight, C. A. (1988) *Biochim. Biophys. Acta 934*, 329–347.

McPherson, P. H., Okamura, M. Y., & Feher, G. (1988) *Biochim. Biophys. Acta 934*, 348–368.

McPherson, P. H., Rongey, S. H., Paddok, M. L., Feher, G., & Okamura, M. Y. (1991) *Biophys. J. 59*, 142a.

Michel, H., Epp, O., & Deisenhofer, J. (1986) *EMBO J. 5*, 2445–2451.

Nabedryk, E., Mäntele, W., Tavitian, B. A., & Breton, J. (1986) *Photochem. Photobiol. 43*, 461–465.

Nabedryk, E., Leonhard, M., Mäntele, W., & Breton, J. (1990a) *Biochemistry 29*, 3242–3247.

Nabedryk, E., Bagley, K. A., Thibodeau, D. L., Bauscher, M., Mäntele, W., & Breton, J. (1990b) *FEBS Lett. 266*, 59–62.

Nabedryk, E., Andrianambinintsoa, S., Berger, G., Leonhard, M., Mäntele, W., & Breton, J. (1990c) *Biochim. Biophys. Acta 1016*, 49–54.

Okamura, M. Y., Isaacson, R. A., & Feher, G. (1975) *Biochim. Biophys. Acta 72*, 3491–3495.

Paddock, M. L., Rongey, S. H., Feher, G., & Okamura, M. Y. (1989) *Proc. Natl. Acad. Sci. U.S.A. 86*, 6602–6606.

Paddock, M. L., McPherson, P. H., Feher, G., & Okamura, M. Y. (1990) *Proc. Natl. Acad. Sci. U.S.A. 87*, 6803–6807.

Paddock, M. L., Rongey, S. H., McPherson, P. H., Feher, G., & Okamura, M. Y. (1991) *Biophys. J. 59*, 142a.

Parson, W. W., & Ke, B. (1982) in *Photosynthesis: Energy Conversion by Plants and Bacteria* (Govindjee, Ed.) p 331, Academic Press, New York.

Rongey, S. H., Paddock, M. L., Juth, A. L., McPherson, P. H., Feher, G., & Okamura, M. Y. (1991) *Biophys. J. 59*, 142a.

Siebert, F., Mäntele, W., & Kreutz, W. (1980) *Biophys. Struct. Mech. 6*, 139–146.

Siebert, F., Mäntele, W., & Kreutz, W. (1982) *FEBS Lett. 141*, 82–87.

Slifkin, M. A., & Walmsley, R. H. (1970) *Spectrochim. Acta 26A*, 1237–1242.

Takahashi, E., & Wraight, C. A. (1990) *Biochim. Biophys. Acta 1020*, 107-111.
Takahashi, E., Maróti, P., & Wraight, C. A. (1991) in *Electron and Proton Transfer in Chemistry and Biology* (Diemann, E., Junge, W., Müller, A., & Ratazczak, H., Eds.) Elsevier Publishers, Amsterdam (in press).
Tavitian, B. A., Nabedryk, E., Mäntele, W., & Breton, J. (1986) *FEBS Lett. 201*, 151-157.
Thibodeau, D. L., Nabedryk, E., Hienerwadel, R., Lenz, F., Mäntele, W., & Breton, J. (1990a) *Biochim. Biophys. Acta 1020*, 253-259.
Thibodeau, D. L., Breton, J., Berthomieu, C., Bagley, K. A., Mäntele, W., & Nabedryk, E. (1990b) in *Reaction Centers of Photosynthetic Bacteria* (Michel-Beyerle, M. E., Ed.) Springer Series in Biophysics, Vol. 6, pp 87-98, Springer, Berlin.
Uhmann, W., Becker, A., Taran, C., & Siebert, F. (1991) *Appl. Spectrosc. 45*, 390-397.
Venyaminov, S. Y., & Kalnin, N. N. (1990) *Biopolymers 30*, 1243-1257.
Wraight, C. A. (1977) *Biochim. Biophys. Acta 459*, 525-531.
Wraight, C. A. (1979) *Biochim. Biophys. Acta 548*, 309-327.

Calcium-Dependent Interaction of Chlorpromazine with the Chloroplast 8-Kilodalton CF_0 Protein and Calcium Gating of H^+ Fluxes between Thylakoid Membrane Domains and the Lumen†

Gisela G. Chiang,‡ Dennis C. Wooten, and Richard A. Dilley*
Department of Biological Sciences, Purdue University, West Lafayette, Indiana 47907
Received January 30, 1992; Revised Manuscript Received April 8, 1992

ABSTRACT: Earlier work suggested that Ca^{2+} ions in the chloroplast thylakoid lumen interact with thylakoid membrane proteins to produce a proton flux gating structure which functions to regulate the expression of the energy-coupling H^+ gradient between localized and delocalized modes [Chiang, G., & Dilley, R. A. (1987) *Biochemistry 26*, 4911-4916]. In this work, one of the phenothiazine Ca^{2+} antagonists, chlorpromazine, was used as a photoaffinity probe to test for Ca^{2+}-dependent binding of the probe to thylakoid proteins. [^{3}H]Chlorpromazine photoaffinity-labels thylakoid polypeptides of M_r 8K and 6K, with generally much less label occurring in other proteins (some experiments showed labeled proteins at M_r 13K-15K). More label was incorporated in circumstances where it is expected that Ca^{2+} occupies the putative H^+ flux gating site, compared to when the gating site is not occupied by calcium. The photoaffinity labeling of the 8-kDa protein was also influenced by the energization level of the thylakoids (less labeling under H^+ uptake energization). The 8-kDa protein was identified by partial amino acid sequence data as subunit III of the thylakoid CF_0 H^+ channel complex. The partial amino acid sequence of the 6-kDa protein (19 residues were determined with some uncertainties) was compared to data in the GCG sequence analysis data base, and no clear identity to a known sequence was revealed. Neither the exact site of putative Ca^{2+} binding to the CF_0 proteolipid nor the site of covalent attachment of the chlorpromazine to the CF_0 component has been identified. Evidence for gating of energy-linked H^+ fluxes by the hypothesized Ca^{2+}-CF_0 gating site came from the correlation between Ca^{2+}-dependent binding of chlorpromazine to the CF_0 8-kDa protein with inhibition of light-driven H^+ uptake into the lumen but no inhibition of H^+ uptake into sequestered membrane domains. When conditions favored a delocalized $\Delta\tilde{\mu}_{H^+}$ coupling mode, less chlorpromazine was bound to the CF_0 structure, and much larger amounts of H^+ ions were accumulated in the lumen. The data support the hypothesis that Ca^{2+} ions act in concert with the 8-kDa CF_0 protein (and perhaps another protein, the 6-kDa polypeptide?) in a gating mechanism for regulating the expression of the energy-coupling H^+ gradient between localized or delocalized coupling modes.

Recent results have been interpreted as supporting the notion that in thylakoids ATP formation appears to be driven by $\Delta\tilde{\mu}_{H^+}$ gradients that are either delocalized (Davenport & McCarty, 1980; Vinkler et al., 1980; Gräber, 1982; Beard & Dilley, 1986, 1988a; Sigalet et al., 1985; Junge, 1987) or localized (Ort et al., 1986; Graan et al., 1981; Horner & Moudrianakis, 1983, 1986; Sigalet et al., 1985; Beard & Dilley, 1986, 1988a; Pick et al., 1987). The localized coupling hypothesis is still controversial, perhaps partly because it is so difficult to propose models which can account for localized energy-coupling proton gradients. However, the data supporting the localized coupling hypothesis are broadly based, and the search goes on for more critical ways to test the hypothesis [cf. Dilley (1990) for a recent review].

A development that strengthens the localized coupling hypothesis, inasmuch as it introduces discrete, controllable processes, is the recent work suggesting that the energy-coupling modes can be reversibly switched or gated between the localized or delocalized modes under the influence of Ca^{2+} ions (Chiang & Dilley, 1987). High levels of KCl or NaCl (≈100 mM) in the thylakoid storage buffer elicit a delocalized cou-

† This work was supported in part by grants from the National Science Foundation and the U.S. Department of Energy.
* To whom correspondence should be addressed.
‡ Present address: Department of Plant Biology, Carnegie Institution of Washington, 290 Panama St., Stanford, CA 94305-4170.

0006-2960/92/0431-5808$03.00/0